A new indirect method of measuring the contents of solid inclusions in liquid aluminium alloys

X. CAO
Department of Metallurgy and Materials, The University of Birmingham, Birmingham B15 2TT, England; Aerospace Manufacturing Technology Centre, Institute for Aerospace Research, National Research Council Canada, 5145 Decelles Avenue, Montreal, Quebec, Canada H3T 2B2
E-mail: Xinjin.cao@cnrc-nrc.gc.ca.

Published online: 5 April 2006

The introduction of derivative methods and the classification of three flow states (i.e. initial transient, steady and terminal transient stages) provide new approaches to understand the filtration behaviors of liquid aluminum alloys during the Prefil Footprinter tests. The effectiveness of the filtration equations of incompressible cake mode can be well identified over some steady stages during the course of the filtration tests. Based on these new findings a new indirect method of measuring the contents of solid inclusions in liquid aluminum alloys is developed using the Prefil Footprinter tests. However, the benchmarks of specific cake resistance should be made for commercial aluminum alloy melts before this method becomes feasible in laboratories and industries. It is found that for a given volume concentration of solid inclusions, lighter inclusions usually lead to higher specific cake resistance, and the heavier solid inclusions reduce the specific cake resistance. For higher quality liquid metal, usually with lower lumped parameter ($\sigma\alpha$), the types of solid inclusions have less influence on specific cake resistance.

Nomenclature

- A Cross-sectional area of the cake and filter (m^2)
- K' A constant characteristic of the bed and fluid properties
- L Thickness of the bed (m)
- L_c Thickness of cake (m)
- L_m Thickness of filter medium (m)
- ΔP Pressure difference or drop across the cake and filter (Pa)
- R_c Resistance of filter cake (m^{-1})
- R_m Resistance of filter medium (m^{-1})
- S_v Specific surface area, i.e. the ratio of particle surface area to volume (m^2/m^3)
- V Volume of filtrate that has passed the filter during time t (m^3)
- W Weight of filtrate that has passed the filter during time t (kg)
- $Q = dV/dt =$ Volumetric flow rate (m^3/s)
- r Capillary radius (m)
- t Filtration time (s)
- u Filtrate velocity (m/s)
- α Density of filtrate (kg/m^3)
- ρ_s Density of solid inclusions (kg/m^3)
- α Specific cake resistance (m/kg)
- μ Viscosity of filtrate (Pa × s or N-s/m^2)
- σ Solid inclusion mass captured per unit filtrate volume (kg/m^3) and
- ε Fraction of voids (voidage or porosity), i.e. volume of voids to total bed volume

1. Introduction

Solid inclusion contents in liquid aluminium alloys have been a main concern for metallurgical industries. There are usually two quantitative methods to measure the inclusion concentrations in molten aluminum alloys: electrical resistance and filtration [1]. Liquid Metal Cleanliness Analyzer (LiMCA), based on the electrical resistance measurement, is thought to provide truly in-line detection of inclusion quantities and sizes, though the equipment is expensive, not portable, and requires a significant amount of maintenance [1–3]. The methods based on the pressure filtration or pre-concentration tests are Porous Disc Filtration Analysis (PoDFA) from Alcan and Liquid Aluminum Inclusions Sampler (LAIS) from Union Carbide

0022-2461
DOI: 10.1007/s10853-006-6977-x

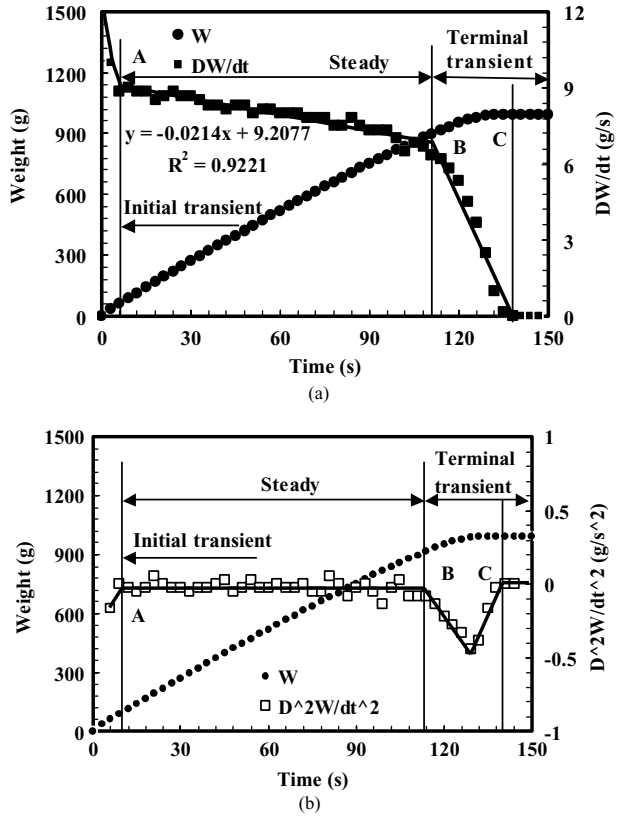

Figure 1 A typical Prefil filtrate weight versus filtration time curve for alloy 4 and their 1st and 2nd derivative curves.

[3]. Pressure filtration operates at pressure levels above the atmospheric. The pressure differential created across the filter medium causes flow of the liquid metal through the filter, leaving an inclusion-rich cake above the filter medium. The metallurgical analyses of the concentrated samples can provide a qualitative and quantitative evaluation of the inclusions though these methods are very expensive, being both time-consuming and effectively offline procedures. In addition, experienced metallurgical technical personnel are required to carry out the inclusion analyses [2].

To produce good quality castings, instantaneous real-time measurement of liquid metal quality is essential to foundries. Over the past decade another portable Pressure Filtration Technique (Prefil Footprinter test) has been introduced to provide both real-time (on-line) representations of melt quality characteristics together with concentrated metallurgical samples for further inclusion evaluation if necessary [4–7]. The method, developed and patented by N-Tech, England, is based on the PoDFA technique combined with a real-time data acquisition system that allows the recording of the filtrate weight versus filtration time profiles while the test is being performed. Comparison of the filtrate weight versus filtration time graph with earlier benchmarks seems to provide a measure of the cleanness of liquid metal. Examination of the material trapped in and above the filter can further confirm the results and extend the interpretation. Recently

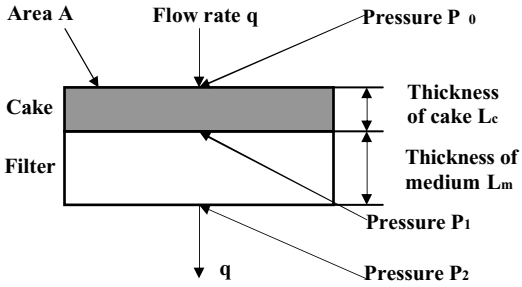

Figure 2 Schematic diagram showing the flow of liquid metal through the cake and filter medium during the pressure filtration test.

the filtrate weight versus filtration time curves have been analyzed for the first time using 1st and 2nd derivative methods [8]. It is interesting to find that there probably exist three phases during the pressure filtration tests. These are initial transient, steady and terminal transient states as shown in Fig. 1 [8]. The analysis of the flow behavior of liquid metal during the Prefil Footprinter tests provides new approaches to understand and compare liquid metal quality [9–13]. To better understand the mechanism of the Prefil Footprinter test, the general equations of cake mode filtration will be introduced in the following section.

2. Filtration equations of cake mode

Filtration is usually used to separate suspended solids from slurry or suspension (here liquid metal) through a filter (medium or barrier). The pores of the filter medium are small enough to prevent the passage of some of the solid particles. As filtration proceeds, some solid material is left behind and forms a cake on the top of the filter medium as schematically shown in Fig. 2 [14–16]. The cake itself serves as a second barrier.

From a study of the flow of liquids through a bed of sand, Darcy proposed the empirical relation in 1856, now well known as Darcy's law [17]:

$$u = \frac{1}{A}\frac{dV}{dt} = K'\frac{\Delta P}{L} \tag{1}$$

Where u is the overall fluid velocity, L the thickness of the bed, ΔP the pressure drop across the bed, K' a constant characteristic of the bed and fluid properties, V the volume of fluid flowing in time t, and A the cross-sectional area of the bed.

Shortly before Darcy's work was published, Poiseuille presented the equation for the flow of liquid through a capillary of circular cross section [17]:

$$\frac{dV}{dt} = \frac{\Delta P \pi r^4}{8\mu L} \tag{2}$$

Where r is the capillary radius and μ the viscosity of the fluid. The Poiseuille equation states that the flow rate of fluid through a capillary is inversely proportional to the viscosity of the fluid.

During the filtration test, the fluid passes through the filter medium, which offers resistance to its passage, under the influence of a force which is the pressure differential across the filter medium. The cake thickness increases from 0 to L_c, corresponding to an increase in filtrate volume collected from 0 to V. According to Darcy's and Poiseuille's laws the flow velocity of the filtrate (u) through the cake and filter medium is proportional to the pressure difference ΔP imposed over the cake and the filter medium; the velocity is inversely proportional to the viscosity of the flowing fluid μ and the resistance of the cake and the filter medium [17–19]:

$$u = \frac{1}{A}\frac{dV}{dt} = \frac{\Delta P}{\mu(R_c + R_m)} \tag{3}$$

The filtration resistance results from the frictional drag on the liquid as it passes through the cake and filter medium [19]. R_m is the resistance of filter medium (m^{-1}) and should be a constant for a given filter medium. If the cake is incompressible, then the cake resistance R_c is directly proportional to the filtrate volume V and inversely proportional to the filter area A [15, 20]:

$$R_c = \alpha\sigma\frac{V}{A} \tag{4}$$

Where α = Specific cake resistance (m/kg), and (σ = Mass of solid cake captured per unit filtrate volume (kg/m^3).

Substituting Eq. 4 into Eq. 3 gives

$$\frac{dV}{dt} = \frac{\Delta P}{\frac{\mu}{A}\left(\alpha\sigma\frac{V}{A} + R_m\right)}, \tag{5}$$

or

$$\frac{dt}{dV} = \frac{\mu\sigma\alpha}{A^2(\Delta P)}V + \frac{\mu R_m}{A(\Delta P)} \tag{6}$$

The specific cake resistance α (m/kg) is introduced as a measure of metal flow resistance. Its physical significance is that it represents the cake resistance to filtration for a unit mass of solid cake deposited per unit filter area [18]. In other words, it represents the pressure drop across the cake at unit filtrate velocity when unit mass solid cake per unit filter area is deposited by unit viscosity melt. Eq. 6 yields a linear function between the inverse volumetric flow rate dt/dV and filtrate volume V [14–20]. To determine specific cake resistance, Eckert et al. [16] once investigated the linear relationships between inverse filtration rate (dt/dV) and cumulative filtrate volume (V) for 1100, 5082 and 7075 aluminum alloys.

Now filtrate volume is replaced by filtrate weight W (g) and the density of the filtrate ρ (kg/m^3) is assumed to be constant, we have

$$\frac{dt}{dW} = \frac{\mu\sigma\alpha}{\rho^2A^2(\Delta P)}W + \frac{\mu R_m}{\rho A(\Delta P)} \tag{7}$$

During the course of filtration the pressure and flow rate may change or remain constant. Thus the mass flow rate dW/dt can be integrated for various modes of filtration such as constant pressure, or constant mass flow rate. If a constant pressure drop (ΔP) across the cake and filter is supposed, and at time $t = 0$, $W = 0$. Thus, we have

$$t = \frac{\mu\sigma\alpha}{2\rho^2A^2(\Delta P)}W^2 + \frac{\mu R_m}{\rho A(\Delta P)}W \tag{8}$$

Eq. 7 also yields a linear function between inverse mass flow rate (dt/dW) and filtrate weight (W). If dt/dW is plotted as a function of W, a straight line should be expected if the filtration operates in an incompressible cake mode. The slope $\frac{\mu\sigma\alpha}{\rho^2A^2(\Delta P)}$ and the intercept $\frac{\mu R_m}{\rho A(\Delta P)}$ can be obtained from the plot.

As shown above, the filtration behavior is directly related with solid inclusion mass captured per unit filtrate volume σ (kg/m^3). If the slope in Eq. 7, or the factor of the second order term in Eq. 8 is known, a new indirect method can be developed to determine the contents of solid inclusions. In this aspect little has ever been investigated up to date using the Prefil Footprinter tests. This work is a first attempt to estimate inclusion concentrations in liquid aluminum alloys using the Prefil Footprinter tests.

3. Experimental procedures

The materials used in the study were nominal cast Al-7/11.5Si-0.4Mg alloys (British designations LM9, LM25 and 2L99) with various Fe, Mn and Ti contents (Table I). The experimental alloys were prepared from Al-30%Si, Al-4%Fe and Al-10%Mn hardener alloys, 99.8%Mg and 99.89%Al ingots. The Al-4%Fe master alloy was melted from 99.88%Fe and 99.89%Al ingots, and the Al-30%Si from 98.7%Si and 99.89%Al ingots. The Al-10%Mn was a commercial master alloy. Alloy 13 (Al-7%Si-0.4%Mg) was a commercial high quality 2L99 alloy ingot that was specially used to calibrate the pressure filtration instrument.

Prior to melting, a clay-graphite crucible (with a capacity of 3 kg) was preheated in a muffle furnace at 450°C overnight. A mass of 3 kg of the experimental alloy was charged to the preheated crucible, melted in an induction furnace, heated to 730 or 760°C and held for 20 min at this temperature to dissolve the charge fully. Disc samples were taken from the melt for chemical analysis of the original alloys using glow discharge spectrometry. Some alloys were subjected to precipitation and sedimentation processing at various precipitation temperatures and times [21–25]. The melting crucible was lifted together with its molten charge from the induction coil and put into a resistance-heated holding furnace where the liquid metal cooled to 600°C and then was held for different sedimentation times from 10 to 240 min to sediment primary α-Al(MnFe)Si phase and inclusions. After the melt has been

TABLE I. Alloy compositions and experimental details used in the work

No	Alloy compositions	Precipitation and sedimentation processing and melting temperatures	Temperatures at filtration
1	Al-11.52Si-0.38Mg-0.57Fe-0.59Mn-0.17Ti	No processing; melted at 730°C	700°C
2	Al-11.52Si-0.38Mg-0.57Fe-0.59Mn-0.17Ti	600°C for 10 min, reheated to 730°C	700°C
3	Al-11.52Si-0.38Mg-0.57Fe-0.59Mn-0.17Ti	600°C for 10 min, reheated to 730°C	700°C
4	Al-11.12Si-0.36Mg-1.14Fe-1.09Mn	No processing; melted at 760°C	700°C
5	Al-11.12Si-0.36Mg-1.14Fe-1.09Mn	No processing; melted at 760°C	720°C
6	Al-11.52Si-0.38Mg-0.57Fe-0.59Mn	600°C for 10 min, reheated to 730°C	700°C
7	Al-11.12Si-0.36Mg-1.14Fe-1.09Mn	600°C for 30 min, reheated to 760°C	720°C
8	Al-11.12Si-0.36Mg-1.14Fe-1.09Mn	600°C for 60 min, reheated to 760°C	720°C
9	Al-11.12Si-0.36Mg-1.14Fe-1.09Mn	600°C for 120 min, reheated to 760°C	720°C
10	Al-11.12Si-0.36Mg-1.14Fe-1.09Mn	585°C for 120 min, reheated to 760°C	700°C
11	Al-11.12Si-0.36Mg-1.14Fe-1.09Mn	600°C for 240 min, reheated to 760°C	720°C
12	Al-7.5Si-0.4Mg-0.5Fe-0.3Mn-0.13Ti	No processing; melted at 760°C	720°C
13	Al-7Si-0.4Mg (commercial UK 2L99)	No processing; melted at 730°C	700°C

Notes. Alloy compositions given in wt.% unless noted otherwise. The holding temperature for alloy 10 was not well controlled, leading to the occurrence of Al solidification during the precipitation and sedimentation processing. After the processing the top clean liquid was decanted from the bottom precipitate-rich material except for alloy 3. Alloys 2 and 3 were reheated in an electric resistance furnace. All other alloys were reheated in an induction furnace after the decantation

held for the preset sedimentation time in the holding furnace, approximately 2.2 kg out of 3 kg of the sedimented melt was carefully decanted to another crucible (preheated at 850°C for about 30 min) to separate the purified melt, leaving approximately 0.8 kg of a precipitate-rich layer at the base of the crucible (for alloy 3 no separation was taken and all the material was reheated in an electric furnace). The precipitate-rich melt was poured into ingot moulds. The purified melt (approximately 2.2 kg) was then reheated to 730 or 760°C. The temperature of the liquid metal was vigilantly controlled during melting, sedimentation and reheating using a *K*-type thermocouple (chromel-alumel) immersed in the melt. The working end of the thermocouple with a wire diameter of approximately 0.5 mm was resistance spot welded and inserted in a silica tube before being immersed in the melt.

The melting crucible was then lifted together with its molten charge and poured approximately 2 kg metal into a crucible preheated for about two hours at 180°C to conduct the Prefil Footprinter test. The crucible was made of a low heat capacity, highly insulating fibrous material equipped with a filter of an average pore size of 90 μm, manufactured by N-Tec. When the metal cooled to either 700°C or 720°C, the pressure chamber was closed and pressure applied to the liquid metal in the crucible, pushing it through the filter. As filtered metal fell into the weigh ladle it was weighed as a function of filtration time and recorded each 3 s. After the pre-set test time (150 s) the pressure was automatically released from the pressure chamber and the filtration test was terminated. During the test of filtration, two stage pressures were employed. A high-pressure of approximately 0.21 MPa (30 psi) was used to start metal flow through the filter at the beginning. When the filtrate weight of more than 20 g was recorded at the load cell the pressure was switched to a low value of approximately 0.08 MPa (12 psi) to maintain metal flow through the filter for the rest of filtration time [26].

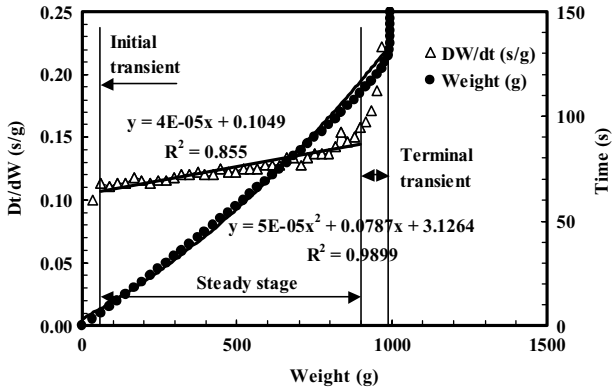

Figure 3 The inverse mass flow rate *dt*/*dW* versus filtrate weight *W* curve for alloy 4 showing the linear relationship only effective for the steady stage.

Alloys 1, 4, 5, 12 and 13 were not subjected to the precipitation and sedimentation processing. After normal melting the liquid metal was directly evaluated using the Prifil Footprinter instrument.

4. Results and discussion

With the introduction of the derivative methods, all the Prefil filtrate weight versus filtration time curves for the experimental alloys have been analyzed and examined [8, 9]. The three stages were identified and listed in Table II. The conventional filtration Eq. 7 was also used to examine the filtration behaviors of liquid aluminum alloys during the Prefil Footprinter tests for all the experimental alloys [11]. It is interesting to find that Prefil Footprinter tests operate mainly in a filtration mechanism of cake mode. The inverse mass flow rate *dt*/*dW* tends to hold a linear relationship with filtrate weight W at the steady stages as shown in Fig. 3. The inverse mass flow rate *dt*/*dW* tends to deviate from the linear relationships with filtrate

TABLE II. Three stages determined using the 1st derivative method and the filtration equations for steady stages

Alloy No	Filtrate weight (g)	Initial transient stage (s)	Steady stage (s)	Terminal transient stage (s)	Linear filtration equations for steady stage	R^2
1	201	0–12	12–150	–	–	–
10	288	0–6	6–150	–	–	–
12	291	0–24	24–150	–	–	–
2	400	0–33	33–150	–	–	–
5	454	0–6	6–51	51–150	Dt/dW = 2.4035E-4W + 0.16491659	0.8687
3	540	0–150	–	–	–	–
9	605	0–138	–	138–150	–	–
8	785	<3	<3–150	–	Dt/dW = 5.877E-5W + 0.16854738	0.8327
7	788	0–6	6–150	–	Dt/dW = 7.412E-5W + 0.16293557	0.8774
6	981	0–6	6–150	–	Dt/dW = 9.933E-5W + 0.10691722	0.8599
4	994	0–6	6–111	111–150	Dt/dW = 4.397E-5W + 0.10486842	0.855
13	1130	0–6	6–150	–	Dt/dW = 5.533E-5W + 0.10267843	0.9325
11	1305	<3	<3–150	–	Dt/dW = 3.287E-5W + 0.09385443	0.9633

TABLE III. Some data used for the calculations in the work [21, 24, 26]

Parameters	Values
Viscosity of filtrate μ	1.19E-3 Pa × s or N-s/m^2
Density of filtrate ρ	2463 kg/m^3
Pressure differential across the cake and filter ΔP	0.08 MPa
Diameter of filtration area d	12.7 mm

TABLE IV. The values of lumped parameter ($\sigma\alpha$) calculated for some experimental alloys.

No	Filtrate weight (g)	$\alpha\sigma$ (m^{-2})
1	201	–
10	288	–
12	291	–
2	400	–
5	454	1.5713E + 09
3	540	–
9	605	–
8	785	3.8422E + 08
7	788	4.8458E + 08
6	981	6.4939E + 08
4	994	2.8746E + 08
13	1130	3.6173E + 08
11	1305	2.1490E + 08

– Not Applicable
(α = Specific cake resistance (m/kg), and
(σ = Solid inclusion mass captured per unit filtrate volume (kg/m^3).

weight W both at the initial transient stages (probably due to the lack of well-formed cakes) and at the terminal transient stages (probably due to the occurrences of partial and/or complete blocking). If both the initial and terminal transient stages disappear the linear relationship between the inverse mass flow rate dt/dW and filtrate weight W tends to hold true over the whole course of the filtration test. For some low filtrate weight liquid metal, however, the deviations of the linear relationship may occur even at the steady stage probably due to the compressibility of the formed cakes caused by oxide films and non-uniform cake thickness. Table II also lists the linear equations between dt/dW and W and their relative coefficients squared for the steady stages of all the experimental alloys if available. When good linear equations between dt/dW and W appear, the Prefil Footprinter tests operate in a filtration mechanism of incompressible cake mode. Clearly, the introduction of derivative methods and the classification of the three phases (i.e. initial transient, steady and terminal transient stages) provide new approaches to understand the filtration behaviors of liquid aluminum alloys during the Prefil Footprinter tests and assume that the incompressible cake mode filtration can be effectively identified over some certain filtration periods. In this case the filtration equations of incompressible cake mode can be effectively applied to understand the filtration behaviors of liquid aluminum alloys.

When the values of slope $\frac{\mu\sigma\alpha}{\rho^2 A^2(\Delta P)}$ for Eq. 7 are obtained for some experimental alloys as shown in Table II, the lumped parameter ($\sigma\alpha$) can be calculated now. The accurate thermophysical data for the experimental alloys around 700–720°C are not available. Table III lists the values used for the estimation in the work [21, 24, 26]. The data of the lumped parameter ($\sigma\alpha$) calculated are shown in Table IV. Though the specific cake resistance (σ) is not known for all the experimental alloys, the values of lumped parameter ($\sigma\alpha$) are the indicative of inclusion types and concentrations in liquid aluminum alloys [16]. Fig. 4 shows the relations between specific cake resistance (α) and solid inclusion mass captured per unit filtrate weight (σ) for some experimental alloys. For a given value of lumped parameter ($\sigma\alpha$), higher specific cake resistance corresponds to lower inclusion concentrations. In the work the lumped parameter ($\sigma\alpha$) is not well correlatively with the values of filtrate weight probably due to the differences of alloy compositions and the methods of liquid metal processing as shown in Table I.

Usually industrial aluminum alloys are dilute or very dilute solution due to its low inclusion concentrations. In this case, solid inclusion mass captured per unit filtrate volume σ (kg/m^3) can be approximately considered to be

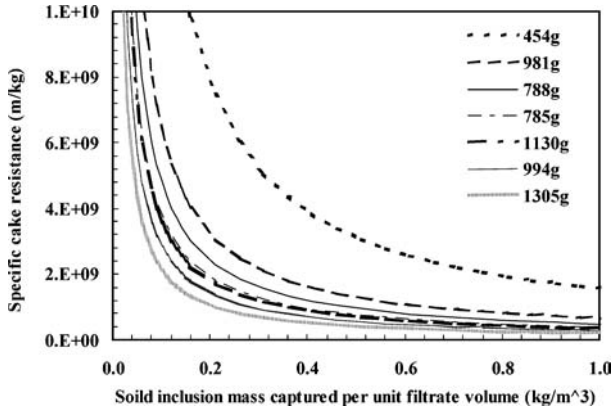

Figure 4 Effect of solid inclusion mass captured per unit filtrate volume on specific cake resistance for some experimental alloys.

inclusion mass concentration per unit volume of liquid metal. If solid inclusions are expressed in volume concentration (%), the relationships between specific cake resistance (α) and inclusion volume concentrations (%) are shown in Fig. 5 according to the decreased order of the values of lumped parameter ($\sigma\alpha$). Here the densities of the solid inclusions are categorized into four values 2500, 3000, 3500 and 4000 kg/m^3, which cover almost most solid inclusion types typically encountered in aluminum alloys such as SiO_2 2660, MgO 3580, Al_2MgO_4 3640, γ-Al_2O_3 3200, α-Al_2O_3 3980, primary α-$Al_{15}(FeMn)_3Si_2$ 3379 kg/m^3, etc. [21, 22, 24]. It is interesting to find that inclusion types have some influence on the values of specific cake resistance for a given volume concentration of solid inclusions. Lighter inclusions lead to higher specific cake resistance. Vice versa, heavier solid inclusions reduce the values of specific cake resistance. However, the types of solid inclusions have less influence on specific cake resistance with decreased values of lumped parameter ($\sigma\alpha$). Usually higher quality liquid metal should have lower values of lumped parameter ($\sigma\alpha$). Thus for higher quality liquid metal, the types of solid inclusions have less influence on the specific cake resistance. As stated above the specific cake resistance α (m/kg) is introduced as a measure of metal flow resistance. Its physical significance is that it represents the flow resistance to filtration for a unit mass of solid cake per unit filter area [18]. This parameter is known to be a function of filter media, alloy system, liquid metal treatment, inclusion type and concentration [16, 17]. Prefil Foorprinter tests usually use special filter media made by N-Tec. Therefore, the specific cake resistance is mainly related to the liquid metal itself and can be used to indicate liquid metal quality.

With the introduction of derivative methods and the classification of three flow phases (i.e. initial transient, steady and terminal transient stages), the filtration behaviors of incompressible cake mode can be identified from the Prefil Footprinter tests. If incompressible cake mode holds true the values of lumped parameter ($\sigma\alpha$) can be obtained. It is clear that an indirect method of measuring solid inclusion contents in aluminum melts can be devel-

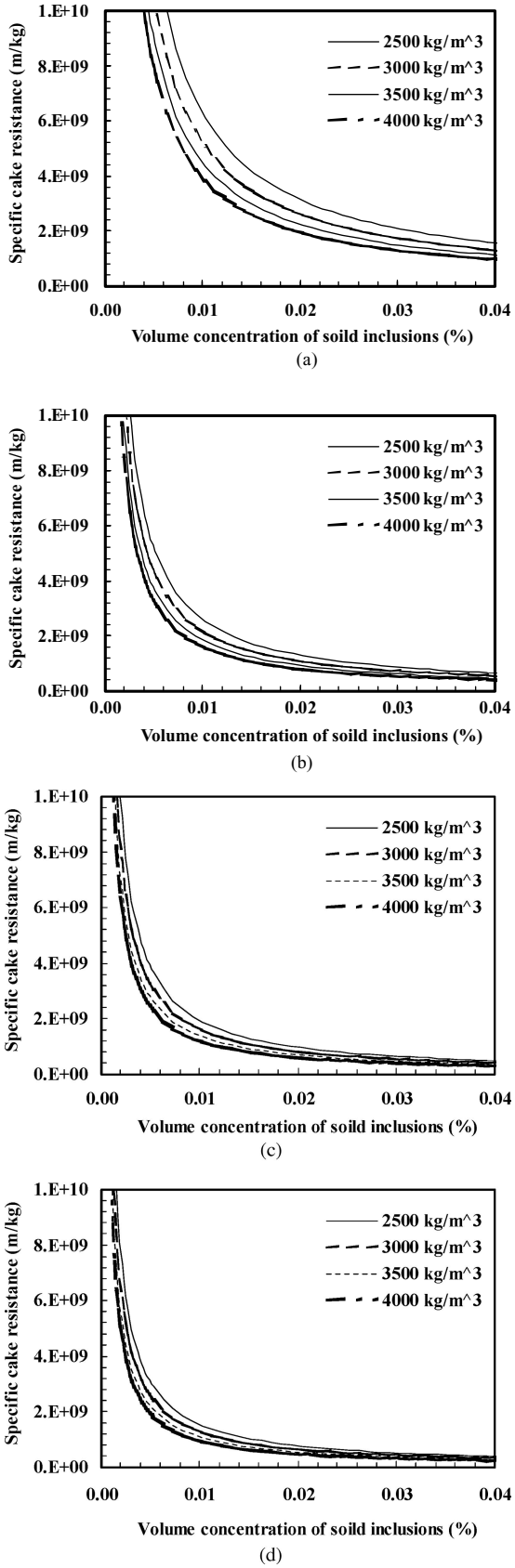

Figure 5 Effect of volume concentrations and densities of solid inclusions on specific cake resistance for experimental alloys (a) 5, (b) 6, (c) 7, (d) 8, (e) 13, (f) 4 and (g) 11.

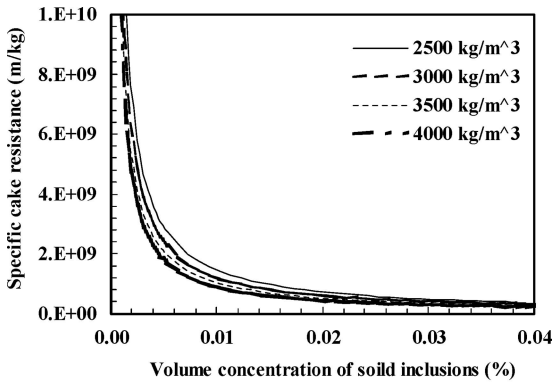

(e)

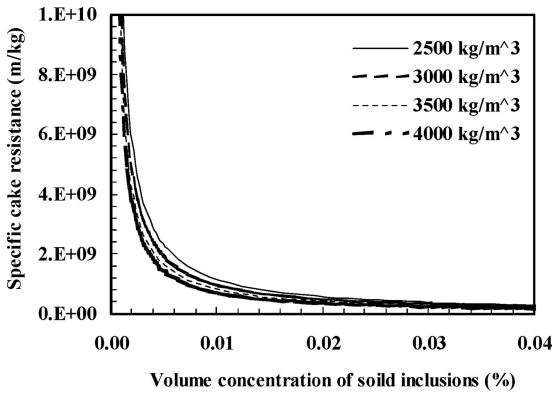

(f)

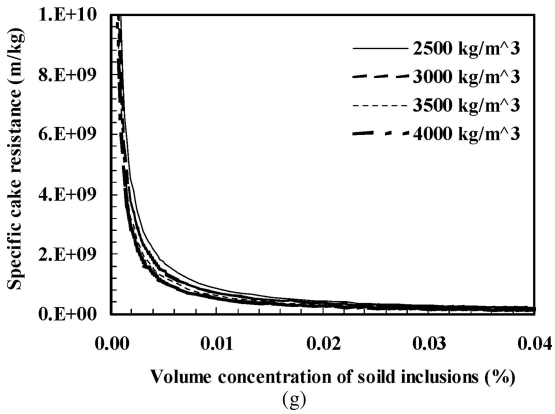

(g)

Figure 5 Continued

oped if specific cake resistance is available. In principle the specific cake resistance can be calculated from the specific surface area S_v, voidage ε, and particle density ρ_s using the following equation [20, 27]:

$$\alpha = \frac{5S_v^2(1-\varepsilon)}{\rho_s \varepsilon^3} \tag{9}$$

In practice, however, lack of data for specific surface area S_v and voidage ε are a major stumbling block due to the complexity of solid inclusions in the formed cake. According to its definition as shown in Eq. 9, the specific cake resistance seems to relate with all properties of the formed cakes, i.e. alloy system, inclusions type, concentration, shape, size, and particle packing in the cake. The distribution of solid inclusions in the cake in turn depends on such factors as the concentration of solid inclusions, velocity of liquid through the cake, rate of filtration, filtration pressure, and may be altered by vibrations [27]. The specific cake resistance, therefore, is beset with far more uncertainty. In addition, commercial aluminum alloys usually contain various kinds of solid inclusions. Even so the benchmarks of specific cake resistance should be investigated for commercial aluminum alloy melts in the future. Much work, therefore, remains to be carried out in this field. The establishment of standard data for different aluminum alloys will also aid predicting the filtration behaviors and evaluate liquid metal quality.

5. Conclusions

The introduction of derivative methods and the classification of three flow phases (i.e. initial transient, steady and terminal transient stages) provide new approaches to understand the filtration behaviors of liquid metal during the Prefil Footprinter tests. The effectiveness of the filtration equations of the incompressible cake mode can be well identified over some steady stages during the course of the filtration tests. Based on these new findings a new indirect method of measuring the concentrations of solid inclusions in aluminum melts is developed using the Prefil Footprinter tests. However, the benchmarks of specific cake resistance should be made for commercial aluminum alloy melts before this method becomes feasible in laboratories and industries. For a given volume concentration of solid inclusions, lighter inclusions usually lead to higher specific cake resistance, and the heavier solid inclusions reduce the specific cake resistance. For higher quality liquid metal, usually with lower lumped parameter ($\sigma\alpha$), the types of solid inclusions have less influence on specific cake resistance.

Acknowledgements

The author is greatly indebted to his supervisor Professor John Campbell for the experiments conducted in the casting laboratory at the University of Birmingham, Birmingham, B15 2TT, England.

References

1. L. A. GODLEWSKI and J. W. ZINDEL, *AFS Trans.* **109** (2001) 315.
2. A. A. SIMARD, F. DALLAIRE, J. PROULX and P. ROCHETTE, in Light Metals (eds.), R. D. PETERSON (The Minerals, Metals & Materials Society, Warrendale, PA, 2000) p. 739.
3. A. SIMARD, J. PROULX and D. PAQUIN, in International AFS Conference on Molten Aluminium Processing, Lake Buena Vista, FL, USA (2001).
4. P. G. ENRIGHT, in Proceedings of Conference 'Ensuring the Highest Quality and Reliability in Light Alloy Castings', Suttow Coldfield, UK (1996), p. 6.1.
5. P.G. ENRIGHT, Equipment Installation and Service Manual: Prifil Footprinter® Series 2 – Aluminium Version, N-Tec, Birmingham, UK, Jan. 1997.

6. P. G. ENRIGHT and I. R. HUGHES, *Foundryman* **89** (11) (1996) 390.
7. P. ROCHETTE and A. A. SIMARD, *Aluminium* **76** (2000) 20.
8. X. CAO, *Scripta Materialia* **52** (2005) 839.
9. X. CAO, *Mater. Sci. Eng. A*, **403** (2005) 101.
10. X. CAO, *ibid*., **403** (2005) 94.
11. X. CAO and M. JAHAZI, *ibid*., **408** (2005) 234.
12. X. CAO and M. JAHAZI, *Mat. Sci. Technol*., **21** (2005) 1192.
13. X. CAO, in "Simulation of Aluminium Shape Casting Processing," edited by Q. G. Qang, M. J. M. Krane and P. D. Lee, TMS (The Minerals, Metals & Materials Society, Warrendale, PA, 2006), in press.
14. D. APELIAN. In Proceedings of Materials Solutions Conference'98 on 'Aluminum Casting Technology', 1998, edited by M. Tiryakioglu and J. Campbell (ASM International, OH, USA) p. 153.
15. C. E. ECKERT, R. E. MILLER, D. APELIAN and R. E. MUTHARASAN, in "Light metals", edited by J. P. McGeer (The Metallurgical Society, Warrendale, PA, 1984) p. 1281.
16. C. E. ECKERT, R. MUTHARASAN, D. APELIAN and R. E. MILLER, in "Light Metals", edited by The Metallurgical Society/AIME (The Metallurgical Society, Warrendale, PA, 24–28 Feb. 1985) p. 1225.
17. M. J. MATTESON and C. ORR, in "Filtration Principles and Practices", 2nd edn (Marcel Dekker Inc., New York, 1987) p. 133.
18. A. RUSHTON, A. S. WARD and R.G. HOLDICH, in "Solid Liquid Separation Technology" (Weinheim, Germany, 1996) p. 33.
19. N. P. CHEREMISINOFF, in "Liquid Filtration", 2nd edition (Butterworth-Heinemann, Boston, 1998) p. 59.
20. C. O. BENNETT and J. E. MYERS, in "Momentum, Heat, and Mass Transfer", 3rd edn (McGRAW-HILL Book Company, New York, 1982) p. 224.
21. X. CAO, PhD Thesis, School of Metallurgy and Materials, The University of Birmingham (2001).
22. X. CAO and J. CAMPBELL, *Metall. Mater. Trans. A* **34A** (2003) 1409.
23. X. CAO and J. CAMPBELL, *Mater. Sci. Tech.* **20** (2004) 514.
24. X. CAO, N. SAUNDERS and J. CAMPBELL, *J. Mater. Sci.* **39** (2004) 2303.
25. X. CAO and J. CAMPBELL, *Metall. Mater. Trans. A* **35A** (5) (2004) 1425.
26. M. LOVIS, Private Communications (October 2004).
27. D. B. PURCHAS, in "Industrial Filtration of Liquids", 2nd edn (Leonard Hill Books, London, 1971) p. 423.

Received 9 March
and accepted 12 September 2005